ISSN 1063-7788, Physics of Atomic Nuclei, 2018, Vol. 81, No. 5, pp. 588–594. © Pleiades Publishing, Ltd., 2018.
Original Russian Text © D.N. Grozdanov, N.A. Fedorov, V.M. Bystritski, Yu.N. Kopach, I.N. Ruskov, V.R. Skoy, T.Yu. Tretyakova, N.I. Zamyatin, D. Wang, F.A. Aliev, C. Hramco, A. Gandhi, A. Kumar, S. Dabylova, E.P. Bogolubov, Yu.N. Barmakov, 2018, published in Yadernaya Fizika, 2018, Vol. 81, No. 5, pp. 548–554.

NUCLEI
Experiment

Measurement of Angular Distributions of Gamma Rays from the Inelastic Scattering of 14.1-MeV Neutrons by Carbon and Oxygen Nuclei

D. N. Grozdanov[1),2)], N. A. Fedorov[1),3)*], V. M. Bystritski[1)], Yu. N. Kopach[1)], I. N. Ruskov[1),2)], V. R. Skoy[1)], T. Yu. Tretyakova[4)], N. I. Zamyatin[1)], D. Wang[1),5)], F. A. Aliev[1),6)], C. Hramco[1),7)], A. Gandhi[8)], A. Kumar[8)], S. Dabylova[1)], E. P. Bogolubov[9)], and Yu. N. Barmakov[9)]

Received January 11, 2018

Abstract—The results obtained by measuring the angular and energy distributions of gamma rays originating from the inelastic scattering of 14.1-MeV neutrons by carbon and oxygen nuclei are presented. The measurements in question were performed by the tagged-neutron method in a beam of an ING-27 standard portable neutron generator. The angular distributions of gamma rays emitted by the 2^+ state of ^{12}C at 4.43 MeV and the 3^- state of ^{16}O at 6.13 MeV were obtained.

DOI: 10.1134/S106377881805006X

1. INTRODUCTION

The TANGRA (TAgged Neutron and Gamma RAys) project at the Joint Institute for Nuclear Research (JINR, Dubna) is aimed primarily [1, 2] at studying in detail fast-neutron scattering off atomic nuclei by means of the tagged-neutron method. Measurement of angular $n\gamma$ correlations in the inelastic scattering of 14.1-MeV neutrons provides additional information about the mechanism of interaction between a target nucleus and a projectile nucleon and about the effective nucleon–nucleon potential [3]. Information about processes of this type is substantially poorer than data available for reactions induced by the inelastic scattering of charged particles off atomic nuclei. A comparison of inelastic neutron and proton scattering is of interest for theoretical studies in the realms of nuclear physics and nuclear astrophysics, since this makes it possible to explore the isospin symmetry of nucleon–nucleon interactions. Interest in $(n, n'\gamma)$ reactions on light and medium-heavy elements is also dictated by the need for refining experimental data obtained earlier, since such reactions are widely applied in geology in determining the elemental composition of rocks [4, 5]. In nuclear power engineering, these reactions are necessary for describing neutron-breeding chains and are also of importance in creating instruments for revealing hidden hazardous substances [6, 7].

The tagged-neutron method is based on the detection of 3.5-MeV alpha particles produced in the reaction

$$d + t \to \alpha + n \qquad (1)$$

and emitted in a direction that is nearly opposite to the neutron-emission direction. The neutron energy is then 14.1 MeV. The reaction products are detected in coincidence with characteristic nuclear gamma-ray radiation originating from inelastic neutron scattering by target nuclei. These reactions can schematically be represented as

$$A(n, n')A^* \xrightarrow{\gamma} A. \qquad (2)$$

It follows that, by fixing the direction of alpha-particle emission, one can reconstruct the neutron-emission direction—that is, tag neutrons. In practice, neutron tagging is accomplished by means of a position-sensitive alpha-particle detector embedded in a neutron generator. Knowledge of the number of tagged neutrons incident to a target, the number of

[1)]Joint Institute for Nuclear Research, Dubna, Moscow oblast, 141980 Russia.
[2)]Institute for Nuclear Research and Nuclear Energy, Bulgarian Academy of Sciences, Sofia, BG-1784 Bulgaria.
[3)]Moscow State University, Moscow, 119991 Russia, Россия.
[4)]Skobeltsyn Institute of Nuclear Physics, Moscow State University, Moscow, 119991 Russia.
[5)]Xi'an Jiao Tong University, Xi'an, China.
[6)]Institute of Geology and Geophysics of Azerbaijan National Academy of Sciences, Baku, Azerbaijan.
[7)]Institute of Chemistry of the Academy of Sciences of Moldova, Chisinau, Republic of Moldova.
[8)]Banaras Hindu University, Varanasi, India.
[9)]All-Russia Research Institute of Automatics (VNIIA), Moscow, 127055 Russia.
[*]E-mail: na.fedorov@physics.msu.ru

$n\gamma$ coincidences, target dimensions, and the detection efficiency for gamma rays of characteristic radiation from nuclei permits correctly determining the differential cross section for inelastic neutron scattering by nuclei of the isotopes being studied that leads to the excitation of specific levels. The possibility of monitoring the flux of tagged neutrons with a high efficiency and thereby substantially reducing the contribution of background events to resulting gamma-ray spectra is an important advantage of the tagged-neutron method.

In [8], our group reported on the results obtained by measuring the angular distribution of gamma rays from the inelastic scattering of 14.1-MeV neutrons by ^{12}C nuclei at the TANGRA setup whose detecting system relied on NaI(Tl) crystals and which involved a shielding collimator for the neutron beam. The use of the tagged-neutron method enabled us to improve the accuracy of the measurements, and this was of paramount importance since the data available in the literature were markedly different. A specific choice of setup geometry allowed the first ever measurements for angles of gamma-rays emission that were smaller than 10°. Measurements with carbon targets were repeated in order to test the new system in question. Below, we present the gamma-ray angular distributions measured in the $(n, n'\gamma)$ reactions on ^{12}C and ^{16}O nuclei.

2. EXPERIMENTAL SETUP

The layout of the TANGRA experimental setup is shown in Fig. 1. As a source of 14.1-MeV neutrons, the setup employs an ING-27 portable neutron generator operating in a continuous mode, which ensures the acceleration of deuterons to an energy of 80 to 100 keV and their focusing on a tritium target. The maximum intensity of the neutron beam created by the generator is 5×10^7 s^{-1} in 4π geometry. Alpha particles of energy 3.5 MeV are recorded by a 64-pixel silicon detector embedded in the generator, characterized by a pixel size of 6×6 mm, and located at a distance of 100 mm from the tritium target. Gamma rays are detected by 18 scintillation detectors based on BGO crystals 76 mm in diameter and 65 mm in thickness. The gamma-ray detectors are arranged in a horizontal plane along a circle of radius 750 mm with a step of 14° in the angle. In contrast the earlier experiment reported in [8], the configuration used here features no additional passive collimation of the neutron beam incident to the target, and this made it possible to reduce the distance between the neutron source and the sample under study to 125 mm. Background events are selected by the time-of-flight method: the incident-neutron energy (14.1 MeV) and the distances both from the tritium target of the generator to the irradiated carbon (oxygen) sample and from the sample to the gamma-ray detectors are known. Therefore, events lying in a narrow time interval whose beginning is specified by the alpha particle from the reaction in (1) are selected for a further analysis. This makes it possible to accomplish an efficient discrimination in time of flight between gamma rays and neutrons that hit the gamma-ray detector. A computer combined with two analog-to-digital converters (ADC), ADCM-16, is used in the acquisition of data and their preliminary analysis [9].

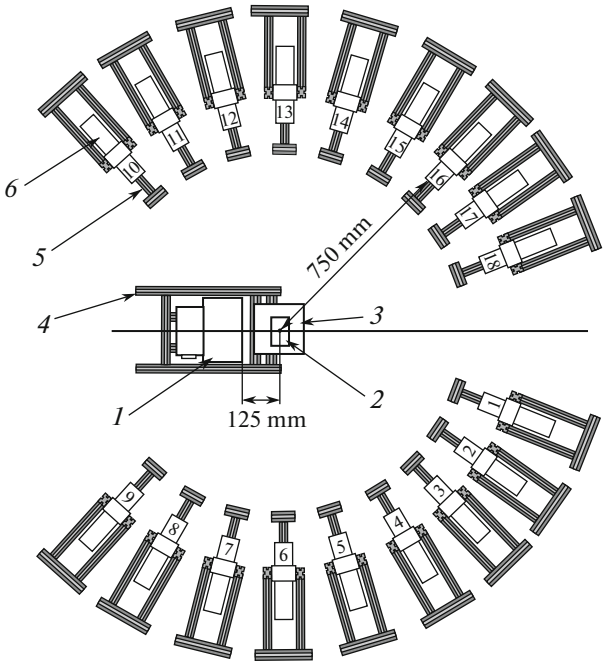

Fig. 1. Layout of the TANGRA experimental setup: (*1*) ING-27 neutron generator, (*2*) target, (*3*) target holder, (*4*) aluminum frame, (*5*) tables for gamma-ray detectors, (*6*) gamma-ray detectors numbered from 1 to 18.

Before the beginning of data acquisition with the samples being studied, the beam from the neutron generator was aligned with the cental axis of the setup. A two-coordinate strip silicon detector (profilometer) that consists of 16 overlapping strips (eight vertical and eight horizontal ones), which eventually yield 64 square zones (pixels) of size length 15 mm, are used to measure spatial features of 64 tagged neutron beams. Fast neutrons are detected in the profilometer owing to the occurrence of the reactions ^{28}Si$(n,p)^{28}$Al and ^{28}Si$(n,\alpha)^{25}$Mg. Figure 2 shows the positions of the ING-27 generator and profilometer in measurements of the neutron-beam shape.

Carbon and glass (primarily formed by SiO_2) blocks $10 \times 10 \times 5$ cm in size were used as targets in our experiments devoted to studying inelastic fast-neutron scattering by carbon and oxygen. The sample

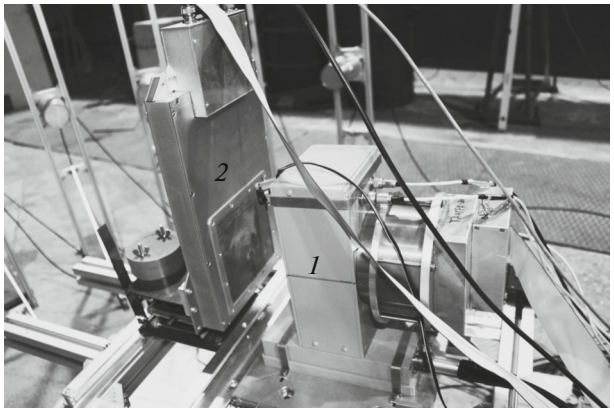

Fig. 2. Measurements of the neutron-beam shape: (*1*) ING-27 generator and (*2*) profilometer.

thickness along the neutron-beam axis was 5 cm. The choice of sample dimensions was based on the results of the simulation performed in [8]. Also, measurements of neutron scattering by oxygen were performed by employing a water target (placed in a container $10 \times 10 \times 10$ cm in size).

3. ANALYSIS OF EXPERIMENTAL DATA

Signals from the alpha-particle and gamma-ray detectors of the TANGRA setup were digitized by means of ADCMs and were logged onto the computer hard disk, whereupon they were analyzed by constructing time and amplitude spectra of events in which detected neutrons and gamma rays were separated in time of flight. As an example, Fig. 3 shows the time spectra of events recorded by the gamma-ray detectors arranged at the angles of 1° and 130° with respect to one of the neutron beams. In contrast to [8], where the analysis of data was performed on the basis of coincidences with the signal from the central pixel of the alpha-particle detector, coincidences with 36 pixels of the alpha-particle detector were taken into account in the present experiment. The time distribution in Fig. 3 exhibits two peaks: peak *1*, which owes its existence to the detection of characteristic gamma-ray radiation from an excited nucleus, and peak *2*, which corresponds to the detection of neutrons that hit the gamma-ray detector.

The energy spectra of events occurring in the time window corresponding to gamma rays (peak *1* in Fig. 3) are constructed for each combination of coincidences between the alpha-particle and gamma-ray detectors by employing the energy calibration of the gamma-ray detectors. Since the gamma-ray detectors are positioned in the horizontal plane, the angle between the emission direction of a photon recorded

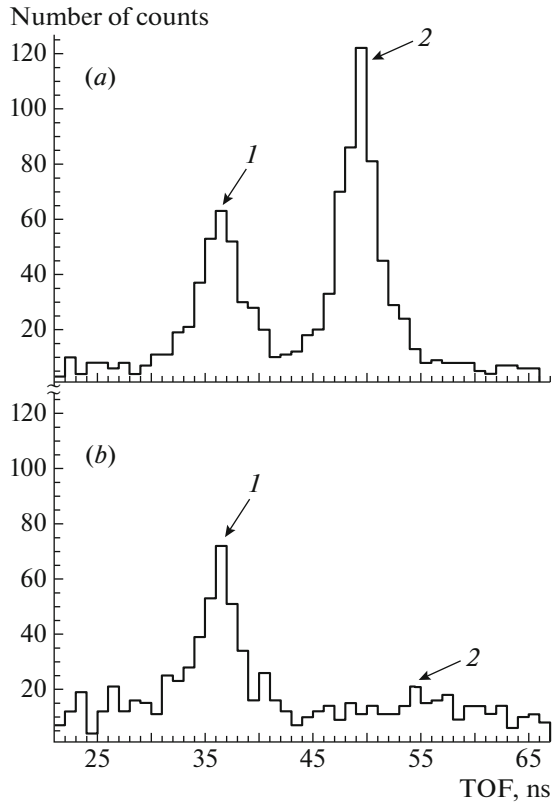

Fig. 3. Time spectra of signals from the gamma-ray detectors: (*a*) time spectrum recorded by the gamma-ray detector no. 1, which is positioned at an angle of 1° with respect to one of the tagged-neutron beams, and (*b*) analogous spectrum from detector no. 9, which is positioned at an angle of 130° with respect to the same beam. Peaks *1* and *2* are associated with gamma rays and neutrons, respectively.

by a gamma-ray detector and the axis of the tagged-neutron beam is only slightly dependent on the vertical coordinate of the alpha-particle detector (y coordinate) and is determined by the horizontal coordinate of the respective pixel of the alpha-particle detector (x coordinate). In performing a data analysis, all pixels of the alpha-particle detector were therefore grouped in the y coordinate, whereby eight strips in the x coordinate were formed. The sample positions and dimensions were chosen in such a way that they were covered by a 6×6 matrix of pixels. At the same time, a 4×6 matrix (four pixels in the x coordinate and six pixels in the y coordinate) were used in the analysis. The edge strips in the x coordinate were discarded, since, for them, a large asymmetry of the counting rate in the gamma-ray detectors situated on the right and on the left of the sample was observed, which was probably associated with gamma-ray absorption in the sample itself. This is not the whole story, however. Since the gamma-ray detectors nos. 1 and 18 proved to be within the region of tagged beams, the present

analysis did not include data from those detectors or the respective xy pixels forming direct neutron beams hitting the aforementioned detectors.

From gamma-ray energy spectra obtained for each strip under analysis, one extracts information about the number of events corresponding to gamma-ray radiation upon the transition of a nucleus from a specific excited state to a state at a lower energy. As a rule, one takes into account only events that lie within the peak of total absorption of the photon energy in the detector or the peak of single emission of a 0.511-MeV annihilation photon.

An anisotropy parameter $W(\theta)$ is introduced in order to describe quantitatively the anisotropy of the angular distribution of gamma rays. This parameter is defined as the ratio of the number of events detected at an angle θ to the number of events detected at an angle of 90°. The experimental angular distributions of gamma rays are approximated by an expansion in terms of Legendre polynomials in the form

$$W(\theta) = 1 + \sum_{i=2}^{2J} a_i P_i(\cos\theta), \qquad (3)$$

where a_i are expansion coefficients, J is the multipole order of the gamma transition, and the summation index i runs through even values exclusively.

4. RESULTS

The inelastic scattering of 14.1-MeV neutrons by ^{12}C nuclei leads to the excitation of only one state that decays thereupon via the emission of a 4.43-MeV photon of $E2$ multipolarity. The other excited states are unstable with respect to nuclear transitions. The angular distribution of gamma rays associated with this transition is given in Fig. 4 for events within the total-absorption peak. That the number of these points is greater than the number of the detectors (see Fig. 1) and that the angular interval between them is smaller than the angular interval between the gamma-ray detectors are a feature peculiar to the tagged-neutron method, which makes it possible to employ not only neutrons emitted along the setup axis but also neutrons emitted within all angles allowed by the aperture of the alpha-particle detector in the generator.

The coefficients a_i in the expansion in terms of Legendre polynomials in expression (3) are listed in Table 1 along with the results reported in [10–12]. The results of the present experiment and the coefficients from [8] are given together with statistical deviations. In order to take into account the systematic errors of the measurements, it is necessary to perform additional simulations and measurements, which are now under way. This involves estimating

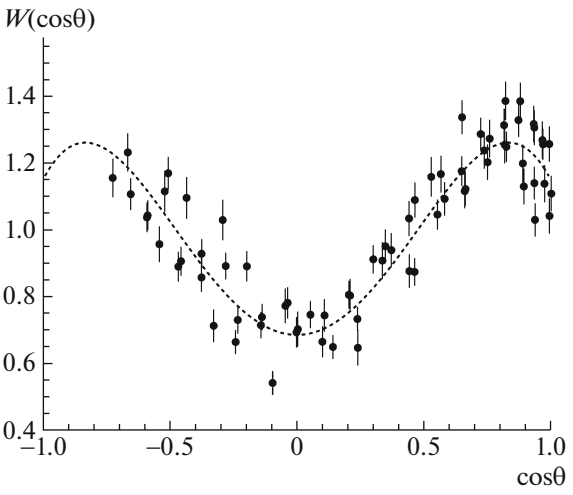

Fig. 4. Angular distribution of 4.43-MeV gamma rays originating from the inelastic scattering of 14.1-MeV neutrons by ^{12}C nuclei.

the contribution of neutron rescattering and gamma-ray absorption in the sample and the effect of finiteness of solid angles, which are determined by the widths of the tagged beams and by the diameters of the gamma-ray detectors, as well as taking into account the difference in the gamma-ray detection efficiency under condition of different counting rates. The inclusion of several tagged beams in the analysis made it possible to enlarge substantially the accumulated data sample, but complicated the processing of experimental data. Within the statistical measurement errors, our results agree with their counterparts obtained earlier. The results at small angles of gamma-ray emission are of importance. The point is that, in evaluated-data libraries, the anisotropy parameters of the angular distribution of 4.43-MeV gamma rays from the $(n, n'\gamma)$ reaction on ^{12}C nuclei do not include the Legendre polynomial of fourth degree, and this leads to a sizable difference between the results of model calculations and experimental data in the region of angles smaller than 45°.

Table 1. Coefficients in the expansion of the angular distribution of gamma rays from the $(n, n'\gamma)$ reaction on ^{12}C nuclei in terms of Legendre polynomials

References	a_2	a_4
Anderson (1958) [10]	0.36 ± 0.04	-0.20 ± 0.05
Benveniste (1960) [11]	0.36 ± 0.08	-0.39 ± 0.09
Spaargaren (1971) [12]	0.40 ± 0.04	-0.37 ± 0.06
Bystritsky (2016) [8]	0.34 ± 0.03	-0.33 ± 0.03
Our study	0.42 ± 0.02	-0.27 ± 0.02

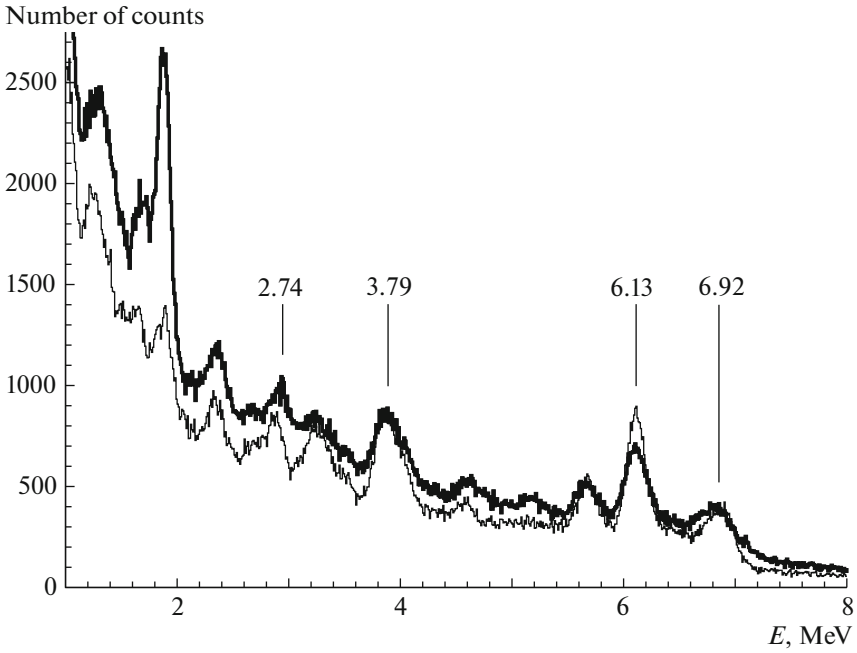

Fig. 5. Energy spectra of gamma rays from the $(n, n'\gamma)$ reactions on (thick line) glass and (thin line) water targets.

The spectrum of excited states in the ^{16}O nucleus has a more complicated structure than the spectrum of excited states in the ^{12}C nucleus, and the respective experimental data reflect this circumstance. Figure 5 shows the energy spectra of gamma rays from the $(n, n'\gamma)$ reaction on targets from glass, which consists primarily of SiO_2, and from water. In either spectrum, the peak at the energy of 6.13 MeV stands out most pronouncedly; this peak corresponds to the transition of $E3$ multipolarity from the state of spin–parity $J^\pi = 3^-$ to the ground state, $0^+_{\text{g.s.}}$ ($3^- \to 0^+_{\text{g.s.}}$), in the ^{16}O nucleus. A peak at the energy of 6.92 MeV manifests itself at higher energies; this peak may owe its existence to the transition from the next excited state, whose quantum numbers are $J^\pi = 2^+$. It is more difficult to interpret the structure of the spectrum for E^* below 6 MeV. In the case of scattering on glass, gamma rays from the $(n, n'\gamma)$ reaction on silicon nuclei make a sizable contribution to the 1.7-MeV resonance that is present in the ^{16}O nucleus and which is due to the transition from the 2^- state at 8.87 MeV to the 1^- state at 7.12 MeV. The peaks in the spectra at 2.74 and 3.79 MeV may result from the excitation of higher lying states of ^{16}O and correspond to the $2^-(8.87\ \text{MeV}) \to 3^-(6.13\ \text{MeV})$ and $2^+(9.84\ \text{MeV}) \to 0^+(6.05\ \text{MeV})$ gamma transitions. However, the resonance in the resulting spectra at the energy of 3.8 MeV may also be due to the deexcitation of the ^{13}C nucleus produced in the reaction $^{16}\text{O}(n, \alpha)^{13}\text{C}$ [13]. Annihilation photons originating from the production of electron–positron pairs in the target material also contribute to the structure of the spectrum in this energy range.

From an analysis of events corresponding to the peak of the total absorption of 6.13-MeV gamma rays, we obtained the anisotropy parameter W as a function of the angle θ. The respective experimental values and the analytic approximation by expression (3) are shown in Fig. 6. The coefficients a_i in the expansion in terms of Legendre polynomials are given in Table 2 along with the coefficients obtained in the present study upon approximating experimental results from [13] and data quoted in the database of the CENTRE FOR PHOTONUCLEAR EXPERIMENTS DATA at Skobeltsyn Institute of Nuclear Physics (SINP, Moscow State University) [14]. It is noteworthy that, in relation to experiments that studied inelastic neutron scattering by carbon, data on the angular distribution of gamma rays from the scattering of 14-MeV neutrons by ^{16}O nuclei are scanty. Data of our present experiment agree with the results of earlier measurements, but have substantially smaller errors. The contribution of high-degree polynomials is of particular interest, since the behavior of the anisotropy in question is of importance not only for simulations and practical applications but also for a theoretical description of inelastic neutron scattering. In that case, a high multipole order of the transitions involved leads to a more complicated angular dependence, which the existing theoretical approaches have not yet reproduced even qualitatively [13].

Table 2. Coefficients in the expansion of the angular distribution of gamma rays from the $(n, n'\gamma)$ reaction on ^{16}O nuclei in terms of Legendre polynomials (the values of a_i were obtained by approximating data on the angular distribution of gamma rays from [13, 14])

References	a_2	a_4	a_6
Kozlowski (1965) [14]	0.2 ± 0.3	-0.3 ± 0.5	-0.7 ± 0.5
Morgan (1964) [14]	0.34 ± 0.04	0.01 ± 0.06	-0.04 ± 0.06
McDonald (1966) [13]	0.22 ± 0.08	-0.05 ± 0.10	-0.32 ± 0.08
Our study	0.34 ± 0.02	0.10 ± 0.02	-0.26 ± 0.08

5. CONCLUSIONS

The inelastic scattering of 14.1-MeV neutrons by carbon and oxygen nuclei has been studied at the TANGRA setup by the tagged-neutron method with the aid of a beam from a standard ING-27 portable neutron generator. Data obtained with several tagged-neutron beams have been included in the data analysis. This made it possible to enlarge the sample of accumulated experimental data and to perform the first ever measurement of the gamma-radiation anisotropy with a resolution higher than eight points per angular interval of 10°.

We have obtained the angular distribution of gamma rays emitted from the first excited state (2^+ state at 4.43 MeV) of the ^{12}C nucleus. The values found above for the coefficients in the expansion of the anisotropy function in terms of Legendre polynomials agree with the results of earlier measurements. Data obtained for the first time at gamma-ray emission angles smaller than 10° with respect to the axis of incident-neutron beam are of importance.

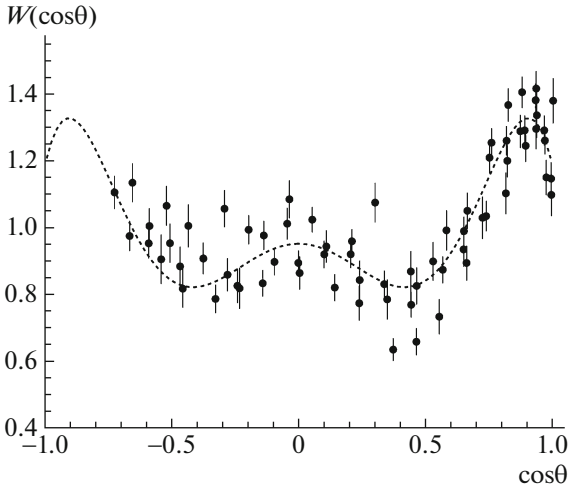

Fig. 6. Angular distribution of 6.13-MeV gamma rays originating from the inelastic scattering of 14.1-MeV neutrons by ^{16}O nuclei.

The angular distribution of gamma rays emitted from the 3^- excited state of ^{16}O at 6.13 MeV has been measured to a high degree of precision. The anisotropy parameters of gamma radiation originating from $(n, n'\gamma)$ reactions at the incident-neutron energy of 14.1 MeV have been found experimentally for the first time.

ACKNOWLEDGMENTS

This work was supported in part by the Russian Foundation for Basic Research (project no. 16-52-45056).

REFERENCES

1. I. N. Ruskov, Yu. N. Kopatch, V. M. Bystritsky, V. R. Skoy, V. N. Shvetsov, F.-J. Hambsch, S. Oberstedt, R. Capote Noy, P. V. Sedyshev, D. N. Grozdanov, I. Zh. Ivanov, V. Yu. Aleksakhin, E. P. Bogolubov, Yu. N. Barmakov, S. V. Khabarov, A. V. Krasnoperov, et al., Phys. Proc. **64**, 163 (2015).
2. V. M. Bystritsky, V. Valkovich, D. N. Grozdanov, A. O. Zontikov, I. Zh. Ivanov, Yu. N. Kopach, A. R. Krylov, Yu. N. Rogov, I. N. Ruskov, M. G. Sapozhnikov, V. R. Skoy, and V. N. Shvetsov, Phys. Part. Nucl. Lett. **12** 325 (2015).
3. W. Hauser and H. Feshbach, Phys. Rev. **87**, 366 (1952).
4. V. Yu. Alekhakhin, V. M. Bystritsky, N. I. Zamyatin, E. V. Zubarev, A. V. Krasnoperov, V. L. Rapatsky, Yu. N. Rogov, A. B. Sadovsky, A. V. Salamatin, R. A. Salmin, M. G. Sapozhnikov, V. M. Slepnev, S. V. Khabarov, E. A. Razinkov, O. G. Tarasov, and G. M. Nikitin, Nucl. Instrum. Methods Phys. Res., Sect. A **785**, 9 (2015).
5. U. Waldschlaeger, Spectrochim. Acta, B **61**, 1115 (2006).
6. S. Pesenti, G. Nebbia, M. Lunardon, G. Viesti, D. Sudac, K. Nđ, S. Blagus, and V. Valković Nucl. Instrum. Methods Phys. Res., Sect. A **531**, 657 (2004).
7. V. M. Bystritsky, V. V. Gerasimov, V. G. Kadyshevsky, A. P. Kobzev, A. A. Nozdrin, Yu. N. Rogov, V. L. Rapatsky, A. B. Sadovsky, A. V. Salamatin, M. G. Sapozhnikov, A. N. Sissakian, I. V. Slepnev, V. M. Slepnev, V. A. Utkin, N. A. Zamyatin, and A. N. Peredery, et al., Phys. Part. Nucl. Lett. **5**, 441 (2008).

8. V. M. Bystritsky, D. N. Grozdanov, A. O. Zontikov, Yu. N. Kopach, Yu. N. Rogov, I. N. Ruskov, A. B. Sadovsky, V. R. Skoy, Yu. N. Barmakov, E. P. Bogolyubov, V. I. Ryzhkov, and D. I. Yurkov, Phys. Part. Nucl. Lett. **13**, 504 (2016).
9. Description of ADCM-16. http://afi.jinr.ru/-ADCM16-LTC.
10. J. D. Anderson, C. C. Gardner, J. W. McClure, M. P. Nakada, and C. Wong, Phys. Rev. **111**, 572 (1958).
11. J. Benveniste, A. C. Mitchell, C. D. Schrader, and J. H. Zenger, Nucl. Phys. **19**, 448 (1960).
12. D. Spaargaren and C. C. Jonker, Nucl. Phys. A **161**, 354 (1971).
13. W. J. McDonald, J. M. Robson, and R. Malcolm, Nucl. Phys. **75**, 353 (1966).
14. T. Kozlowski, W. Kusch, and J. Wojtkowska, http://cdfe.sinp.msu.ru/cgi-bin/exf2htm?-LINK=30081004; T. L. Morgan, J. B. Ashe, and D. O. Nellis, http://cdfe.sinp.msu.ru/cgi-bin/exf2htm?-LINK=12695006.